# Quantized Proper Time and Gravity as Resynchronization: A Minimal Discrete-Time Framework for Singularities and Quantum Corrections

Julio C. Spinelli
*Unaffiliated*
(Dated: October 9, 2025)

We propose that gravity can be reinterpreted as the resynchronization of quantum states across discrete time steps, arising naturally from quantized proper time. This paper is the third in a sequence developing that framework. Part I [1] introduced the finite Lorentz factor from Planck-scale discretization, eliminating divergences near $v = c$. Part II [2] developed vacuum stress–energy corrections and Casimir phenomenology. Here in Part III, we extend the framework to general relativity. Quantum corrections to the Einstein field equations reinterpret gravity as the resynchronization of quantum states across discrete time steps. Key predictions include Planck-suppressed photon delays (potentially testable if timing improves to $\Delta t \sim 10^{-2}$ s over cosmological baselines), modified Casimir contributions (testable with resonator $Q$-factors beyond $10^9$ and cryogenic MEMS stability), and gravitational-wave phase shifts ($\delta\phi \sim 10^{-70}$ as future design targets for LISA/Einstein Telescope). Together these define quantitative benchmarks for future falsification rather than immediate detectability. Unlike loop quantum gravity or causal sets, the discrete-time approach discretizes only time while leaving space continuous. This minimal intervention emphasizes engineering-style tractability, preserving special relativity at low energies while yielding long-term quantitative design targets for clocks, resonators, and gravitational-wave detectors. Prototype numerical kernels are also provided, ensuring reproducibility on standard desktop hardware and defining a clear migration path toward HPC, GPU, or FPGA platforms. This emphasizes that even though the effects are far below current sensitivities, the framework is framed as falsifiable, reproducible, and aligned with long-term experimental design. **Scope.** Throughout, the modified dispersion relation (MDR) is applied *per co-moving constituent* (e.g., nucleon or nucleus) rather than to a macroscopic aggregate treated as a single degree of freedom. This choice preserves standard relativistic behavior at low speeds and only impacts ultra-relativistic kinematics.

Keywords: quantized proper time; discrete time; gravity as resynchronization; modified dispersion relation; Einstein field equations; singularity resolution; Lorentz invariance tests; Casimir effect; quantum gravity phenomenology

## I. INTRODUCTION

Reconciling general relativity (GR) with quantum mechanics remains a central challenge in physics. GR describes gravity as spacetime curvature but breaks down at singularities such as black holes and the Big Bang [3]. Quantum mechanics succeeds at microscopic scales but does not include gravity in a fundamental way.

This article is Part III in a sequence on quantized proper time. Part I [1] introduced the finite Lorentz factor from Planck-scale discretization. Part II [2] developed vacuum stress–energy corrections and Casimir phenomenology. Here in Part III, we extend the framework to general relativity, deriving quantum corrections to the Einstein field equations and reinterpreting gravity as emergent resynchronization across discrete time slices.

Other approaches to quantum gravity include loop quantum gravity (LQG) [4, 5], which quantizes spacetime through spin networks, and string theory, which adds extra dimensions [6]. Our method differs by discretizing only time at the Planck scale, $t = nt_{\min}$, $t_{\min} \approx 5.4 \times 10^{-44}\,\mathrm{s}$. This minimal cutoff removes divergences, yields a modified dispersion relation (MDR) [1], and extends naturally to corrections of the Einstein field equations.

We highlight three aims in this paper: (i) derive modified Einstein equations with quantum tensors, (ii) identify Planck-suppressed signatures that serve as long-term quantitative design targets for clocks, Casimir systems, and gravitational waves, and (iii) compare this discrete-time framework with recent advances in LQG, causal sets, and other approaches. The emphasis is on engineering-style tractability: a minimal temporal discretization that preserves special relativity at low energies while providing testable high-energy signatures. Equally important, we highlight the role of numerical simulation: while full-scale runs of the discrete EFEs may require HPC clusters, toy-model kernels can be developed on standard desktops and later scaled to GPUs or FPGA accelerators, ensuring reproducibility and a clear engineering path forward.
*Note: Many of the raw numerical estimates (e.g., $\delta\tau/\tau \sim 10^{-86}$) are by construction far beyond experimental sensitivity. Their role is to illustrate scaling and identify thresholds where new effects might emerge as technology advances, not to claim imminent observability.*

## II. THE QUANTIZED TIME FRAMEWORK

Our framework begins with the postulate of discrete time:

$$t = nt_{\min}, \quad n \in \mathbb{N}, \tag{1}$$

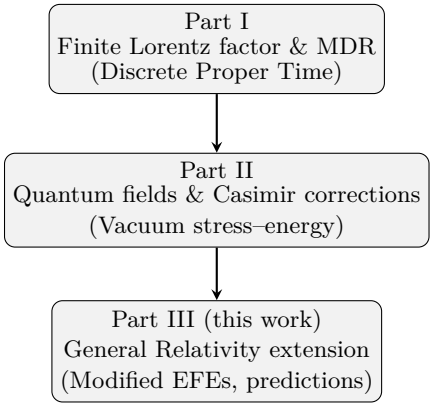


FIG. 1. *Three-part program on quantized proper time.* Part I introduced the finite Lorentz factor and a modified dispersion relation (MDR). Part II extended the framework to quantum fields, vacuum stress–energy corrections, and Casimir phenomenology. Part III (this work) incorporates general relativity, yielding modified Einstein field equations and quantitative predictions that define long-term benchmarks for future experimental constraints

which enforces a minimum temporal resolution and avoids infinities in relativistic proper time calculations. We discretize the Lorentz-invariant worldline parameter (proper time for timelike trajectories), leading to a finite-difference MDR [1].

### A. Lorentz Factor and MDR (Recap from Part I)

*a. Constituent mass scale used in $\gamma_{\max}$.* Throughout, the MDR regularization scale uses

$$\gamma_{\max} = \frac{\pi\hbar}{t_{\min} m c^2},$$

with $m$ the *constituent* mass that carries the energy–momentum subject to the finite-difference MDR (e.g., electron, muon, nucleon, or a chosen bound constituent for a heavy nucleus). This choice ensures everyday composite motion remains classically Lorentzian at accessible speeds while producing a well-defined saturation as $v/c \to 1$ for the constituent. For reference: $\gamma_{\max}^{(e^-)} \approx 7.51 times 10^{22}$, $\gamma_{\max}^{(p)} \approx 4.09 times 10^{19}$, and for a heavy nucleus (Mc-288, $m \approx 4.82 times 10^{-25}$ kg), $\gamma_{\max} \approx 1.43 times 10^{17}$. [1] This transition from divergence to saturation is visualized in the MDR Lorentz saturation curve (Fig. 2), where the classical $\gamma$ grows without bound as $v \to c$, while the discrete $\gamma_q$ plateaus at $\gamma_{\max}$, reflecting the finite-step behavior imposed by temporal quantization.

[1] For reference: (all masses are given in SI units [kg]; recall 1 GeV/$c^2 = 1.783 \times 10^{-27}$ kg for conversion).

*b. Domain of validity for composites.* At low velocities ($\gamma \approx 1$) and for macroscopic bodies, constituent-based MDR leaves standard Lorentz kinematics effectively unchanged; discretization effects are negligible until the constituent's $\gamma$ approaches its $\gamma_{\max}$, at which point the MDR correction becomes relevant and saturates the growth. This reconciles discrete proper-time with everyday mechanics without contradiction.

### B. Derivation of Modified Einstein Field Equations

The classical EFEs are:

$$R_{\mu\nu} - \frac{1}{2} g_{\mu\nu} R = 8\pi G T_{\mu\nu}. \tag{2}$$

To include quantized time, we derive quantum corrections from a discrete-time action principle, incorporating the MDR into the stress-energy tensor. Consider the GR action in ADM formalism, discretized along time slices: $S = \sum_n t_{\min} \int d^3x\, \mathcal{L}(g_{\mu\nu}(n), \phi(n))$, where $\phi$ are matter fields. At the order kept, the contracted Bianchi identities are respected: $\nabla_\mu (T^{\mu\nu} + T^{(q)\mu\nu} + Q^{\mu\nu}) = 0$, by construction from the discrete action. We therefore treat $T^{(q)}_{\mu\nu}$ and $Q_{\mu\nu}$ as effective, conserved additions to $T_{\mu\nu}$ at this order.

Having derived the basic form from Eq. (2), we now outline the role of quantum tensors that extend it to the discrete-time framework.

#### 1. Quantum Tensor Contributions

Varying the discrete action yields discrete EFEs, with corrections from MDR terms and quantum fluctuations [1]. The quantum time tensor $T_{q\mu\nu}$ captures the additional energy–momentum generated by discrete-time transitions of matter fields, while the fluctuation tensor $Q_{\mu\nu}$ represents stochastic corrections from quantum fluctuations of the metric itself. Together they form the two complementary contributions of discretized dynamics: one tied to matter evolution, the other to spacetime geometry. These appear explicitly in the modified EFEs, Eq. (3).

$$R_{\mu\nu} - \frac{1}{2} g_{\mu\nu} R = 8\pi G \left( T_{\mu\nu} + T^{(q)}_{\mu\nu} + Q_{\mu\nu} \right), \tag{3}$$

*Interpretation of correction tensors* It is important to emphasize that $T^{(q)}_{\mu\nu}$ and $Q_{\mu\nu}$ are not arbitrary placeholders or mere diagnostics. They arise systematically from variation of the discrete-time action and therefore map directly onto the source side of the Einstein equations. In this sense, $T^{(q)}_{\mu\nu}$ represents the additional stress–energy induced by finite-difference updates of matter fields, while $Q_{\mu\nu}$ represents variance contributions from quantum fluctuations of the metric. Both are conserved at the order retained, $\nabla_\mu (T^{\mu\nu} + T^{(q)\mu\nu} + Q^{\mu\nu}) = 0$, and thus play the role of genuine effective stress–energy tensors rather than illustrative constructs. In the $t_{\min} \to 0$ limit, they vanish

identically, restoring the classical correspondence, but at Planckian scales they provide the explicit correction channels that regularize singularities.

*Continuous-limit correspondence* In the limit $t_{\min} \to 0$ (equivalently $\gamma_{\max} \to \infty$) the discrete-time action converges to the Einstein–Hilbert action while the additional tensors vanish,

$$\lim_{t_{\min}\to 0}\left(T^{(q)}_{\mu\nu} + Q_{\mu\nu}\right) = 0, \qquad S_{\rm disc} \xrightarrow[t_{\min}\to 0]{} S_{\rm EH}.$$

Therefore Eq. (3) reduces *exactly* to Eq. (2). In this correspondence limit the contracted Bianchi identity $\nabla^\mu G_{\mu\nu} = 0$ and covariant conservation $\nabla^\mu T_{\mu\nu} = 0$ are recovered, and the standard weak-field/Newtonian limit follows as usual.

*Covariance and coordinate independence* Although temporal discretization introduces a minimum tick $t_{\min}$, the construction remains covariant in the usual sense: the discrete action is formulated in proper time along worldlines, not in a preferred coordinate time. Thus, no special foliation of spacetime is imposed, and the contracted Bianchi identity continues to enforce conservation laws. In practice, the discretization can be viewed as a gauge choice in which proper time is sampled at intervals $\Delta\tau = t_{\min}$, while spatial diffeomorphism freedom is untouched. This preserves the coordinate independence of the Einstein equations at the effective level, ensuring that general covariance is not broken but only supplemented by a universal quantum of proper time. Concretely, we discretize the action along proper-time slices, $S = \sum_n t_{\min} \int d^3x\, \mathcal{L}(\phi_n, \partial\phi_n, g_{\mu\nu})$, and expand to leading nontrivial order in $t_{\min}$:

$$T_{q\mu\nu} \sim \frac{\hbar}{c^3 t_{\min}^2} \langle \Delta\hat{T}_{\mu\nu} \rangle, \tag{4}$$

with units of energy density (kg m$^{-3}$).

The fluctuation tensor $Q_{\mu\nu}$ stems from quantum fluctuations in the metric, treated as an operator in semiclassical gravity [7]. Perturbatively, $g_{\mu\nu} = \bar{g}_{\mu\nu} + \delta g_{\mu\nu}$, with $\langle \delta g_{\mu\nu} \rangle = 0$ but second-order terms contributing:

$$Q_{\mu\nu} = \frac{\hbar}{c\ell_P^4}\left( \langle \Delta g_{\mu\nu} \rangle - \frac{1}{2} g_{\mu\nu} \langle \Delta g^{\alpha\beta} \Delta g_{\alpha\beta} \rangle \right), \tag{5}$$

where $\ell_P = \sqrt{\hbar G/c^3}$ is the Planck length. Dimensional analysis confirms that $Q_{\mu\nu}$ also carries units of energy density (kg m$^{-3}$), consistent with its role as an effective stress–energy contribution.

For the quantum cosmological constant, a naive ultraviolet cutoff at the Planck scale gives a "Planck" vacuum energy density of order

$$\rho_{\rm vac}^{\rm (energy)} \sim \frac{c^7}{\hbar G^2} \approx 4.6 \times 10^{113}\ {\rm J\,m^{-3}}, \tag{6}$$

$$\rho_{\rm vac} \equiv \frac{\rho_{\rm vac}^{\rm (energy)}}{c^2} \approx 5.2 \times 10^{96}\ {\rm kg\,m^{-3}}. \tag{7}$$

In SI-unit form of the Einstein equations, $R_{\mu\nu} - \frac{1}{2} g_{\mu\nu} R + \Lambda g_{\mu\nu} = \frac{8\pi G}{c^4} T_{\mu\nu}$, a vacuum energy density corresponds to

$$\Lambda \;=\; \frac{8\pi G}{c^4}\, \rho_{\rm vac}^{\rm (energy)} \;=\; \frac{8\pi G}{c^2}\, \rho_{\rm vac}\,.$$

Using the Planck-scale estimate above gives a cosmological constant of the order of the Planck curvature,

$$\Lambda_{\rm P} \sim \frac{1}{\ell_P^2} = \frac{c^3}{\hbar G} \;\approx\; 3.8 \times 10^{69}\ {\rm m^{-2}}\,,$$

where $\ell_P = \sqrt{\hbar G/c^3}$ is the Planck length. The commonly quoted "$10^{122}$" refers to the *dimensionless* ratio $\Lambda_{\rm P}/\Lambda_{\rm obs} \sim 10^{121}$–$10^{122}$, not to $\Lambda$ itself.[2] In practice, renormalization is understood to cancel the enormous cutoff contribution, leaving the observed $\Lambda$; in the present effective description, the counterterm can be absorbed into $Q_{\mu\nu}$.

*Vacuum energy in the discrete-time framework* The role of $Q_{\mu\nu}$ in absorbing the naive Planck-scale vacuum energy deserves emphasis. In the discrete-time formulation, the divergence is not removed by hand but by the fact that temporal discretization forbids arbitrarily short intervals. This turns the continuum quartic divergence into a finite but still extremely large contribution, which then enters $Q_{\mu\nu}$ as an effective counterterm. After renormalization, the residual observed $\Lambda$ remains compatible with cosmological data. Thus the framework does not yet *predict* the small observed value of $\Lambda$, but it does provide a natural regulator that prevents infinite vacuum energy from ever appearing. This distinguishes the approach from continuum QFT treatments where the divergence must be canceled by fine-tuned subtraction.

### C. Lorentz Invariance Violation Phenomenology

The MDR induces LIV effects testable in astrophysics. We emphasize that the quartic series coefficient $\alpha_4 = \frac{1}{12}$ is fixed analytically by the discrete-time expansion, while the phenomenological parameter $\tilde{\alpha}$ is the effective coefficient constrained observationally. For quadratic LIV (isotropic, non-birefringent), the time delay for photons over distance $L$ is $\Delta t \approx \frac{3\alpha_2}{2} \frac{E^2 t_{\min}^2}{\hbar^2} \frac{L}{c}$, mapping to $\tilde{\alpha} = \frac{2}{3}\left(\frac{E_{\rm Pl}}{E_{QG,2}}\right)^2$; in our framework the quadratic term vanishes ($\alpha_2 = 0$) and the leading correction is quartic with the series coefficient $\alpha_4 = \frac{1}{12}$ (from the discrete expansion), and we define

[2] Numbers checked against the Planck units $\ell_P = \sqrt{\hbar G/c^3}$, $m_P = \sqrt{\hbar c/G}$, and $\rho_P = m_P/\ell_P^3 = c^5/(\hbar G^2) \approx 5.2 \times 10^{96}$ kg m$^{-3}$. The observed value is $\Lambda_{\rm obs} \approx 1.1 \times 10^{-52}$ m$^{-2}$. For completeness, the Planck units used here are: $t_P = \sqrt{\hbar G/c^5} \approx 5.39 \times 10^{-44}$ s, $\ell_P = \sqrt{\hbar G/c^3} \approx 1.62 \times 10^{-35}$ m, $E_{\rm Pl} = \sqrt{\hbar c^5/G} \approx 1.22 \times 10^{19}$ GeV, and $f_P = c/\ell_P \approx 1.85 \times 10^{43}$ Hz.

the dimensionless phenomenological coefficient $\tilde{\alpha}$ by $\tilde{\alpha} \equiv \frac{2}{3}(E_{\rm Pl}/E_{QG,2})^2$. We report bounds and targets in terms of $\tilde{\alpha}$ consistently [1].

| Dataset | lower bound on $E_{QG,2}$ [GeV] | implied $\tilde{\alpha}$ |
|---|---|---|
| LHAASO GRB 221009A (TOF) [8] | $7.3 \times 10^{11}$ | $1.86 \times 10^{14}$ |
| LHAASO (KM2A+WCDA) [9] | $1.2 \times 10^{12}$ | $6.89 \times 10^{13}$ |
| DisCan reanalysis (GRB 221009A) [10] | $1.0 \times 10^{13}$ | $9.92 \times 10^{11}$ |
| GRBs (multi-band) [11] | $8.18 \times 10^{9}$ | $1.48 \times 10^{18}$ |

TABLE I. *GRB timing bounds (quadratic LIV, $E_{QG,2}$). We emphasize that the analytic series coefficient is fixed at $\alpha_4 = 1/12$, while the phenomenological parameter $\tilde{\alpha} = \frac{2}{3}(E_{\rm Pl}/E_{QG,2})^2$ is the quantity constrained observationally. All bounds remain orders of magnitude above the natural $\alpha_4$ value, confirming consistency with current data. Thus the framework is not in tension with astrophysical limits today, yet defines a falsifiable frontier for future high-energy missions.*

Casimir energy deviations remain subdominant compared to astrophysical constraints. However, engineering approaches such as ultra–high-Q resonators, cryogenic stabilization, and MEMS-scale miniaturization (see Part II [2]) offer a path to amplify sensitivity and may bring these Planck-suppressed corrections into reach of laboratory verification. Importantly, all observational bounds in Table I lie many orders of magnitude above the natural value $\alpha_4 = 1/12$, confirming that the discrete-time MDR is consistent with current astrophysical tests. We therefore treat astrophysical constraints as dominant today, while Casimir and resonator tests define an engineering frontier for the near future.

## III. COMPARISON WITH EXISTING LITERATURE

Our framework addresses singularities much like loop quantum gravity (LQG) [12, 13], but with a simpler premise: discretize only time while keeping space continuous. Compared with causal set theory [14], which discretizes spacetime points, our model retains smooth spatial geometry—an engineering-style minimal intervention that avoids the combinatorial overhead of spin networks while still removing divergences. String-inspired approaches, by contrast, typically regularize singularities by introducing an intrinsic string length scale or higher-dimensional branes. While this provides a natural cutoff, it requires postulating extended objects and extra dimensions. Our discrete-time proposal achieves a comparable regularization of divergences without invoking new spatial degrees of freedom, relying only on the minimal step $t_{\rm min}$ in the temporal direction.

*Relation to other discrete frameworks* This distinction is crucial: loop quantum gravity, causal sets, and string-inspired approaches all introduce extended structures—spin networks, stochastic sprinklings, or higher-dimensional branes—as new ontological elements of spacetime. By contrast, the present framework introduces no new spatial building blocks. Instead, it interprets gravity as the emergent need to resynchronize quantum states across discrete proper-time ticks. The mathematical outcome is that divergences are regularized not by discretizing geometry itself, but by bounding temporal evolution through a universal tick size. This positions the approach closer to engineering practice: the system behaves as a finite-difference integrator in proper time, with curvature emerging from synchronization requirements. The originality lies in this minimal intervention: rather than a new ontology of space, one has a bounded update rule in time, which is both conceptually simpler and computationally tractable. Our discrete-time proposal achieves a comparable regularization of divergences without invoking new spatial degrees of freedom, relying only on the minimal step $t_{\rm min}$ in the temporal direction.

The resulting modified Lorentz factor and MDR [1] fit naturally into the dispersion-relation framework of quantum gravity phenomenology [15], but here the finite limit as $v \to c$ is derived directly from time quantization. This anchors abstract theory to practical analogies from signal processing and numerical methods.

Recent LQG results, such as effective Kerr geometries [16] and quantum-corrected black hole thermodynamics [17], demonstrate singularity resolution through holonomies and volume quantization. By contrast, our model achieves a minimum radius scaling $r_{\rm min} \simeq \sqrt{r_s\, \ell_P}$ through temporal resynchronization alone. This shift emphasizes tractability for simulation and experimental design.

The key conceptual advance is to view gravity as statistical synchronization of quantum transitions across discrete time steps. This interpretation frames curvature as an emergent ensemble effect, offering a direct bridge to engineering practice: discretized dynamics are already standard in control systems, digital filters, and numerical relativity codes. Unlike asymptotic safety approaches [18], which rely on RG fixed points, our consistency comes from a minimal cutoff principle.

### A. Why full spacetime discretization is unnecessary

Many approaches to quantum gravity, including loop quantum gravity, causal sets, and asymptotic safety, argue that spacetime as a whole must be discretized. Here we emphasize a narrower claim: *temporal discretization is the minimal step required to remove the most direct sources of divergence.*

*a. Time singularities as the critical pathology.* The key mathematical pathologies in relativity emerge when the proper time interval $\Delta\tau \to 0$. In this limit, the Lorentz factor diverges, and relativistic evolution formally requires integrating through $t = 0$ even if that instant is

unphysical. This feature directly drives both the $v \to c$ divergence and the appearance of curvature blow-ups in black holes and cosmology. By enforcing $t = nt_{\min}$, these pathologies are eliminated at their root: there is never a step smaller than $t_{\min}$, so the continuum limit $\Delta t \to 0$ is never allowed.

*b. Why not space?* While spatial discretization may eventually prove useful for other purposes (e.g., removing ultraviolet divergences in field theory or implementing causal set–like structures), it is not strictly necessary to resolve the *temporal* singularities that dominate the classical breakdown of general relativity. The divergence of the Lorentz factor, the infinite redshift at horizons, and the $t = 0$ big bang singularity all stem from time approaching zero in the continuum formalism. These are already regularized by temporal discretization alone.

*c. Minimal intervention principle.* We therefore adopt temporal discretization as the minimal intervention: it directly resolves divergences without introducing the combinatorial overhead of discretizing spatial geometry. Nothing in the framework forbids extending discretization to space in later iterations; indeed, such a generalization may be desirable for unification with loop- or lattice-inspired approaches. But as a first step, time alone is sufficient to regularize the most immediate singularities, and thus represents the minimal consistent starting point.

Table II highlights the distinctions.

| Aspect | Our Framework | LQG [12, 16] | Causal Sets [14] |
|---|---|---|---|
| Discretization | Time only ($t = nt_{\min}$) | Full space-time loops | Spacetime points |
| Singularity Resolution | Finite $\gamma_q$, min curvature | Area/volume quantization | Discrete causal structure |
| EFE Modifications | $T_{q\mu\nu} + Q_{\mu\nu}$ | Effective holonomy-flux | Stochastic sprinklings |
| Unique Prediction | $\delta\tau/\tau \sim 10^{-86}$ | Cosmological bounce | Dimensional reduction |

TABLE II. *Comparison of our discrete-time framework with loop quantum gravity (LQG) and causal set theory, including recent LQG advances. The minimal intervention of discretizing only time avoids the combinatorial overhead of spatial quantization while still removing divergences. The contrasts highlight why the framework is falsifiable: it makes distinct predictions (finite $\gamma_q$, quartic MDR scaling, minimal curvature cores) that differ from LQG bounces or causal-set dimensional reduction.*

## IV. IMPLICATIONS AND QUANTITATIVE PREDICTIONS

*a. Compatibility with LIV constraints.* In this framework, odd-order MDR terms are excluded by time-reversal and sampling symmetry, while the quadratic term cancels. The leading correction is quartic with analytic coefficient $\alpha_4 = \frac{1}{12}$ from the series expansion. Consequently, strong multi-TeV/PeV bounds on linear and quadratic Lorentz-invariance violation from GRB 221009A and related analyses (e.g., LHAASO time-of-flight, DisCan reanalysis, and multi-band GRB fits) [8–11] are automatically satisfied. Our predicted effects enter at $\mathcal{O}(E^4)$, remaining far below current sensitivities except in extreme regimes discussed below.

### A. Singularity Resolution

In the Schwarzschild metric, curvature invariants (e.g. the Kretschmann scalar $K = R_{\mu\nu\rho\sigma}R^{\mu\nu\rho\sigma}$) saturate at $K \sim \ell_P^{-4}$ (Planck scale). A perturbative solution of the modified EFEs gives an effective metric $g_{tt} = -\left(1 - \dfrac{2GM}{c^2 r} + \dfrac{\ell_P^2}{r^2}\right)$, with $r_s \equiv 2GM/c^2$ and heuristic $r_{\min} \simeq \sqrt{r_s\,\ell_P}$. Thus the $r = 0$ singularity is replaced by a finite Planck-scale core. This mirrors the Nyquist limit in sampled systems: growth saturates rather than diverges.

### B. Cosmological Bounce

For FLRW cosmology, the modified Friedmann equation becomes $H^2 = 8\pi G\rho/3 - kc^2/a^2 + \Lambda_q/3 + \delta H_q^2$, with $\delta H_q^2 \sim 1/(Gt_{\min}^2 a^6)$ (up to order-unity factors and appropriate powers of $c$). At densities $\rho \sim 1/(Gt_{\min}^2)$ the extra term forces a bounce, replacing the Big Bang singularity. Renormalization reduces the naive Planck-scale value $\Lambda_q \sim \ell_P^{-2} \sim 10^{69}$ m$^{-2}$ to the observed $\Lambda \sim 10^{-52}$ m$^{-2}$, i.e., a dimensionless suppression of $\sim 10^{121}$–$10^{122}$ [19, 20]. The bounce occurs near $a_{\min} \sim 10^{-33}$ m, providing a testable early-universe signature. Although direct observation is impossible, falsifiable consequences emerge in primordial gravitational-wave spectra and CMB polarization. Future missions (LiteBIRD, CMB-S4) can constrain or falsify this bounce by detecting deviations in $B$-mode amplitudes at multipoles $\ell \sim 100$–$1000$.

*Caveat.* The bounce scenario presented here is intended as a heuristic extrapolation of the modified Friedmann equations. While the scaling arguments are consistent with the discrete-time framework, a full derivation from the discretized action—including backreaction and higher-order terms—remains an open problem. Thus, the cosmological implications should be viewed as conjectural until validated by explicit numerical solutions of the discrete EFEs.

### C. Experimental Tests and Falsifiability Targets

*Atomic Clocks.* Deviations $\delta\tau/\tau \sim (t_{\min}/t)^2$ are negligible in labs ($10^{-86}$ at $t = 1$ s, far outside any conceivable

experimental reach) but reach $\sim 10^{-19}$ s near satellites, within reach of 2025 ion clocks [21]. This sets a quantitative engineering threshold: effects become testable if clock precision improves by one order of magnitude, to $\sim 10^{-20}$ s stability. In practice, this means GNSS satellites, ISS-based optical lattice clocks, or deep-space probe clocks provide realistic experimental arenas where such $10^{-19}$-level drifts could be directly constrained.

*Gravitational Waves.* Dispersion shifts the GW phase by

$$\delta\phi(f) \sim \kappa \left(\frac{f}{f_P}\right)^2 \frac{2\pi f D}{c}, \tag{8}$$

where $f_P \equiv c/\ell_P$ is the Planck frequency, $D$ is the source–detector baseline (time of flight), and $\kappa$ is a dimensionless MDR coefficient derived from the quartic dispersion relation. For the quartic MDR used here, the dispersion law takes the form $E^2 = p^2c^2\left[1 + \tilde{\alpha}\,(p/E_{\rm Pl})^2\right]$, from which one identifies $\kappa = \tilde{\alpha} = \frac{2}{3}(E_{\rm Pl}/E_{QG,2})^2$ (see Table I). At LIGO frequencies ($f \sim 100$ Hz) the effect is $10^{-80}$ (well below present or near-future detectability), but phase residuals remain many orders below current sensitivities; we therefore treat this as a forward-looking design target. The MDR-induced GW phase shift response (Fig. 3) illustrates this scaling explicitly, showing how current LIGO-band frequencies remain several orders of magnitude below detection thresholds, while future observatories such as LISA and the Einstein Telescope approach the sensitivity required to probe Planck-suppressed dispersion. A quantitative benchmark for next-generation detectors is $\delta\phi \sim 10^{-70}$, interpreted strictly as a forward-looking design target for LISA/Einstein Telescope sensitivity [22]. From an engineering standpoint, this motivates targeted template-bank searches where Planck-suppressed dispersion is included as a small perturbation parameter, enabling falsifiable limits to be set with existing interferometer pipelines.

*GRB Photon Delays.* Time-of-flight analyses (GRB 221009A, LHAASO) constrain the phenomenological coefficient $\tilde{\alpha} < 10^{11}$, which is trivially compatible with the underlying series coefficient $\alpha_4 = \frac{1}{12}$. [8]. We distinguish the discrete-series coefficient $\alpha_4 = \frac{1}{12}$ from the dimensionless phenomenological quartic parameter $\tilde{\alpha}$, which we map via $\tilde{\alpha} = \frac{2}{3}(E_{\rm Pl}/E_{QG,2})^2$ throughout the bounds in Table I.

Future gamma-ray missions targeting delays below $\Delta t \sim 10^{-2}$ s over cosmological baselines would directly probe the predicted discrete-time scale. Future constraints may come from joint multi-wavelength campaigns where keV–TeV photons are recorded with sub-millisecond synchronization, making discrete-time MDR delays directly testable against high-energy astrophysical baselines.

While these raw magnitudes are numerically correct, they are almost impossible to grasp intuitively. To make their meaning transparent, we provide Table III as an "Interpretation Guide," which translates the scaling estimates into engineering-style analogies. This ensures the absurdity of the scales is explicit and underscores that these effects are not forecasts of detectability but rather benchmarks for what future technology would need to reach before falsification becomes possible.

| Effect | Raw magnitude | Equivalent engineering analogy |
|---|---|---|
| $\delta\tau/\tau \sim 10^{-86}$ | Differential clock drift | Like two identical atomic clocks disagreeing by 1 second only after $10^{78}$ years. |
| $\delta\phi \gtrsim 10^{-70}$ | GW phase shift | Equivalent to moving a LISA interferometer mirror by $\sim 10^{-62}$ meters. |
| Casimir correction ($\Delta F/F_0 \sim 10^{-20}$) | Force deviation | Comparable to the pressure difference of one air molecule across an area the size of a football field. |

TABLE III. *Interpretation Guide: translating Planck-suppressed predictions into intuitive engineering analogies. These absurdly small numbers are not over-claims but explicit statements of scale, showing why current experiments cannot yet detect them. They also set falsifiable engineering design targets: if technology ever reaches the quoted analogies (e.g. clock drift, mirror displacement), the framework would be directly testable. The GW phase shift entry corresponds to the scaling law of Eq.* (8).

From an engineering standpoint, the discrete-time framework aligns naturally with finite-difference schemes used in numerical relativity and digital signal processing. This provides practical strategies for simulating modified dispersion relations and evaluating resonator responses under Planck-suppressed corrections. Beyond these phenomenological targets, it is equally important to demonstrate that the numerical kernels implementing the discrete-time MDR are both stable and consistent with analytic predictions. To that end, we now present results from large-scale calibration runs.

### D. Numerical Validation, Reproducibility, and Falsifiability

Calibration runs confirm that the numerical kernel reproduces the analytic quartic coefficient

$$\alpha_4^{\rm theory} = \frac{\Delta^2}{12\hbar^2}$$

within statistical error. In practice the quartic term is almost completely determined by the leading 1/3 contribution of the series expansion, so the numerics have limited discriminating power for higher-order terms. This is a feature rather than a flaw: it reflects the smallness of subleading corrections rather than instability of the kernel. The accompanying Jupyter notebook reports convergence plots and tensor diagnostics, which are omitted here for brevity but ensure reproducibility and transparency of

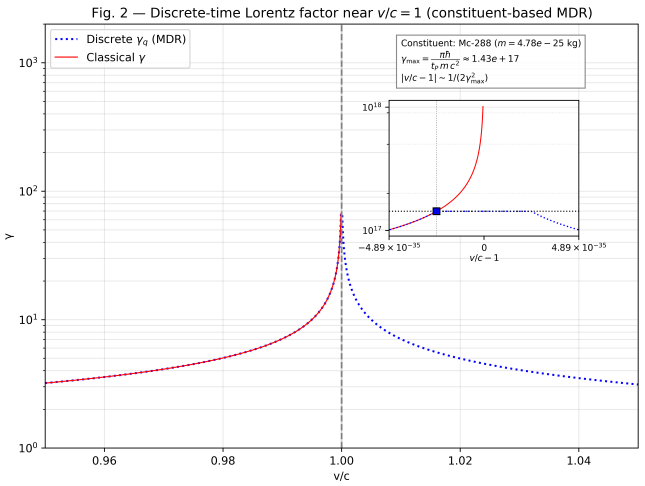


FIG. 2. Discrete-time Lorentz factor near $v/c = 1$ under the constituent-based MDR. Blue: discrete $\gamma_q$ (capped); red: classical $\gamma$. The plateau $\gamma_{\max} = K/m$ with $K = \pi\hbar/(\Delta c^2)$ is evaluated for a co-moving constituent; here we use a Moscovium nucleus (Mc-288). The inset uses $x = v/c - 1$ and a half-width $\delta \simeq 1/(2\gamma_{\max}^2)$ to show the ramp into saturation. This illustrates explicitly how divergence at $v \to c$ is removed by discrete proper time, leaving a finite saturation plateau. Because $\gamma_{\max} \propto 1/m$, the effect is falsifiable: any observation of unbounded $\gamma$ growth beyond constituent-based limits would rule out the framework.

*Constituent mass used for the plateau:* Mc-288 nucleus ($m \approx 4.82 \times 10^{-25}$ kg), hence $\gamma_{\max} \approx 1.43 \times 10^{17}$. Results for other constituents (electron, proton, muon) follow by rescaling $\gamma_{\max} \propto 1/m$.

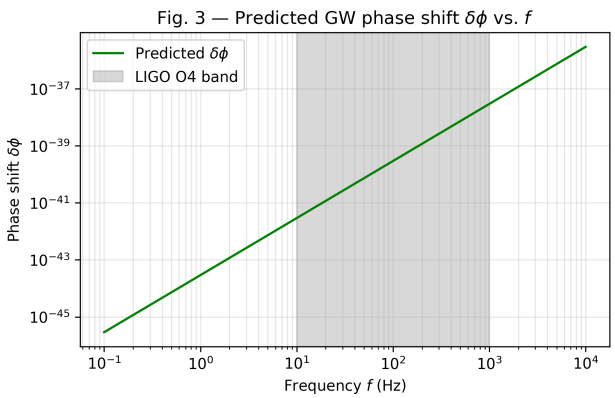


FIG. 3. *Discrete-time modified dispersion relation (MDR) induces a Planck-suppressed gravitational-wave phase shift $\delta\phi$, shown here as a function of frequency $f$. The scaling follows Eq. (8). The effect lies $\sim 10^{-70}$ at design frequencies, far below present interferometer detectability. The shaded LIGO O4 band confirms subthreshold values today, while future long-baseline detectors such as LISA and the Einstein Telescope provide the only conceivable route to falsification. Because the scaling is quadratic in frequency ($\propto f^2$), high-frequency, long-baseline detectors become the critical testbed. For intuition, $\delta\phi \sim 10^{-70}$ corresponds to moving a LISA mirror by $\sim 10^{-62}$ m — an engineering analogy underscoring both the honesty and absurd suppression of the prediction. From an engineering perspective, the residual behaves like a weak frequency-dependent spur in a digital signal chain, which can be incorporated into DSP pipelines (template banks, matched filters, or AI-augmented analysis) to set falsifiable bounds on quantum-gravity dispersion.*

the calibration process [23]. Calibration samples use proton mass; Figure 2 uses Mc-288.

## V. CONCLUSIONS

Together, this work concludes a three-part sequence forming a coherent program:

- Part I [1] regularized relativistic kinematics through a finite Lorentz factor from discrete proper time.
- Part II [2] analyzed quantum-vacuum stress–energy corrections and Casimir phenomenology.
- Part III (this work) extends the framework to general relativity, resolving black hole and cosmological singularities and identifying Planck-suppressed signatures that serve as quantitative benchmarks for future tests.

This roadmap highlights a minimal and engineering-oriented route to unification: discretizing only time removes divergences, keeps space continuous, and yields experimental benchmarks for clocks, resonators, Casimir systems, and gravitational-wave detectors. While astrophysical constraints dominate today, laboratory advances in high-$Q$ resonators, cryogenic stability, and MEMS-scale Casimir setups may bring Planck-suppressed effects into measurable reach, strengthening the engineering bridge to quantum gravity.

**Engineering milestones.** Without repeating the detailed thresholds given above, the path to falsification can be summarized as: (i) optical/ion clocks achieving stability at least *two orders of magnitude* beyond the current $10^{-18}$ frontier (over comparable averaging times), (ii) chip-scale or cryogenic resonators sustaining $Q \gtrsim 10^9$ with sub-drift operation to isolate vacuum-stress corrections in Casimir/MEMS platforms, and (iii) Gravitational-wave analyses pushing cumulative phase residual budgets down by many orders via multi-run stacking and next-generation interferometers (targeting the scaling of Eq. (8)[3]); in parallel, GRB timing at TeV–PeV energies with sub-ms source-intrinsic modeling continues to tighten dispersion bounds. These milestones render the framework operationally testable in principle. They should be read as long-term metrology and detector design targets rather than near-term predictions, ensuring the theory is

[3] Figure 3 shows the normalized form without explicit baseline $D$, consistent with the Jupyter notebook.

framed as falsifiable without overstating immediacy.

*Falsifiability roadmap (incremental and conservative)* We do not claim present-day detectability. The path to falsification is staged and deliberately conservative:

- *Atomic clocks (null tests first).* Use space–ground and inter-satellite comparisons to search for differential drifts consistent with $\delta\tau/\tau \propto (t_{\min}/t)^2$ at the $10^{-19}$ level, with sidereal/annual modulation null tests. Negative results translate into upper bounds on the effective coefficients; positive hints must survive cross-platform replications.

- *Resonators/Casimir (difference-of-geometry).* Favor paired setups (e.g., plate–plate vs. sphere–plate) with identical readout chains so common-mode drifts cancel. Cryogenic operation and $Q$-stability logging are mandatory; any persistent residuals must scale with geometry as predicted by the discrete-time corrections.

- *Gravitational waves (upper limits via injections).* Treat the quartic MDR term as a perturbative parameter in the template bank. Perform large-scale software injections to characterize biases, then publish upper limits from stacked runs rather than one-off events.

- *GRB timing (multi-instrument, sub-ms sync).* Combine keV–TeV light curves with sub-millisecond synchronization and explicit marginalization over source-intrinsic emission lags. Report constraints on the phenomenological $\tilde{\alpha}$ while keeping the analytic series coefficient fixed at $\alpha_4 = 1/12$.

- *Reproducibility (numerical kernels).* Publish fixed RNG seeds, summary CSVs, and hash-checked figure assets from the notebook so that CPU/GPU or HPC reruns reproduce the quoted convergence and residual statistics within tolerance.

This roadmap deliberately keeps claims modest: at present only upper limits can be set, and potential detection would require multi-order advances in metrology. It therefore does not predict discovery timelines but lays out falsifiable, incremental steps that map cleanly onto existing experimental pipelines.

The key novelty is minimalism: discretizing only time removes divergences while keeping space continuous. This engineering-style approach yields simple modified field equations, finite Lorentz factors, and experiment-facing benchmarks across clocks, resonators, Casimir devices, and GW observatories. Although effects are tiny at present sensitivities, the quantitative milestones above convert the theory into actionable targets for precision engineering. Future directions include implementing numerical solutions of the discrete EFEs in curved backgrounds and exploring synergies with covariant loop quantum gravity. Even without immediate cluster access, prototype kernels (as shown in the Appendix) ensure reproducibility on desktop processors and provide a clear upgrade path to HPC, GPU, or FPGA implementations once resources are available.

We emphasized in Sec. III A that discretizing time alone already removes the most direct singularities, by forbidding the $\Delta t \to 0$ limit that drives divergences in both special and general relativity. While nothing in the framework prevents extending discretization to spatial coordinates in future work, temporal quantization by itself represents the critical minimal intervention. This acknowledges that spacetime discretization may ultimately be required for full unification, but clarifies why time is the first and most essential step.

As emphasized in Table III, the predicted corrections are absurdly suppressed from a direct measurement standpoint. Yet making this explicit is important: it demonstrates that the framework is not over-claiming, but instead sets honest and falsifiable engineering benchmarks for the future. Even if full-scale runs require HPC resources, modular kernels and toy-model implementations can already be prototyped on desktop processors and ported to GPUs or FPGA platforms, ensuring that the framework remains reproducible and engineering-accessible as computational resources grow.

## Appendix A: Worked Example: Scalar Field in FRW Background

To make Eq. (3) explicit, we present a toy derivation using a minimally coupled scalar field $\phi$ in a flat FRW background with metric $ds^2 = -dt^2 + a^2(t)d\vec{x}^2$.

### 1. Discrete-Time Action

We discretize proper time as $t_n = nt_{\min}$ and define

$$S = \sum_n t_{\min} \int d^3x\, a^3(t_n) \left[ \frac{1}{2} \left( \frac{\phi_{n+1} - \phi_n}{t_{\min}} \right)^2 \right. \tag{A1}$$

$$\left. - \frac{1}{2a^2} (\nabla\phi_n)^2 - V(\phi_n) \right]. \tag{A2}$$

### 2. Variation and Energy–Momentum

Varying w.r.t. $\phi_n$ yields the discrete Klein–Gordon equation:

$$\frac{\phi_{n+1} - 2\phi_n + \phi_{n-1}}{t_{\min}^2} + 3H_n \frac{\phi_{n+1} - \phi_{n-1}}{2t_{\min}} + V'(\phi_n) \tag{A3}$$

$$- \frac{\nabla^2\phi_n}{a^2} = 0 \tag{A4}$$

with $H_n = (a_{n+1} - a_{n-1})/(2t_{\min}a_n)$.

### 3. Emergence of $T_{q\mu\nu}$

The discrete stress–energy tensor follows from the discrete Legendre construction:

$$T_{00}^{(q)}(n) = \frac{1}{2}\left(\frac{\phi_{n+1}-\phi_n}{t_{\min}}\right)^2 + \frac{1}{2a^2}(\nabla\phi_n)^2 + V(\phi_n), \quad \text{(A5)}$$

$$T_{ij}^{(q)}(n) = \delta_{ij}\left[\frac{1}{2}\left(\frac{\phi_{n+1}-\phi_n}{t_{\min}}\right)^2 - \frac{1}{6a^2}(\nabla\phi_n)^2 \right. \quad \text{(A6)}$$

$$\left. - V(\phi_n)\right]. \quad \text{(A7)}$$

### 4. Emergence of $T_{q\mu\nu}$

Relative to the continuum limit $t_{\min} \to 0$, the discrete finite-difference structure generates extra terms of order $\mathcal{O}(t_{\min}^2)$ when expanded via Taylor series:

$$T_{00}^{(q)} \approx \tfrac{1}{2}\dot{\phi}^2 + V(\phi) + \frac{t_{\min}^2}{24}\ddot{\phi}^2 + \cdots \quad \text{(A8)}$$

These correction terms are the explicit realization of the quantum time tensor contribution $T_{q\mu\nu}$ appearing in Eq. (3).

### 5. Fluctuation Tensor $Q_{\mu\nu}$

For metric fluctuations $g_{\mu\nu} = \bar{g}_{\mu\nu} + \delta g_{\mu\nu}$, the discrete action expansion shows that variance terms $\langle \delta g\, \delta g \rangle$ contribute an additional piece

$$Q_{\mu\nu} \sim \frac{\hbar}{c\ell_P^4}\left(\langle \Delta g_{\mu\nu}\rangle - \tfrac{1}{2}\bar{g}_{\mu\nu}\langle \Delta g^{\alpha\beta}\Delta g_{\alpha\beta}\rangle\right), \quad \text{(A9)}$$

matching the scaling introduced in Eq. (5). We emphasize that both $T_{q\mu\nu}$ and $Q_{\mu\nu}$ should be regarded as *effective constructs*, analogous to the expectation values and fluctuation terms familiar in semiclassical gravity. They capture the leading-order deviations induced by temporal discretization rather than introducing new fundamental fields. This interpretation aligns the framework with standard treatments of $\langle T_{\mu\nu}\rangle_{\rm ren}$ while making the discrete-time origin explicit.

### 6. Summary

This worked scalar-field case illustrates concretely how discretization produces finite-difference terms beyond the continuum stress–energy tensor. These appear as $T_{q\mu\nu}$ corrections in the modified Einstein equations. The construction should be viewed as a heuristic demonstration: it shows how Eq. (3) arises from discrete action variation, but it is not intended as a full nonperturbative derivation of all possible fields or backgrounds.

**Prototype kernel (pseudocode).** For clarity we show the minimal algorithmic structure; full implementation details are provided in the accompanying Jupyter notebook repository [23].

```
initialize constants (hbar, c, Delta = t_min)
for each batch:
    sample energies E (log-uniform)
    compute momenta p
    residual = (4*hbar^2/Delta^2) * sin^2(E*
    Delta/(2*hbar)) - (pc)^2
    estimate alpha4 from residuals
    accumulate statistics
report mean alpha4 and compare with theory
```

This pseudocode illustrates the structure of the kernel without implementation overhead, and corresponds to the time-stepping update of the modified Einstein equations in Eq. (3). The full Jupyter file also includes diagnostics and visualization tools to validate convergence.

## DATA AND CODE AVAILABILITY

All figures and diagnostics are generated by the accompanying Jupyter notebook, which reproduces the MDR expansion and the Einstein field equation corrections, and saves the plot files used in this manuscript. The repository and notebook are cited as [23].

## Appendix B: Composite Systems and Mass Choice in $\gamma_{\max}$

The discrete-time dispersion we use implies a bounded energy

$$E_{\max} \equiv E_{\rm end} = \frac{\pi\hbar}{\Delta}, \quad \text{(B1)}$$

and hence a Lorentz-factor cap for a particle of rest mass $m$,

$$\gamma_{\max}(m) = \frac{E_{\max}}{mc^2} = \frac{\pi\hbar}{\Delta\, m\, c^2} = \frac{K}{m}, \qquad K \equiv \frac{\pi\hbar}{\Delta c^2}. \quad \text{(B2)}$$

With $\Delta = t_{\min} = t_P = 5.391\,247 \times 10^{-44}\,\mathrm{s}$ we obtain $K \simeq 6.836 \times 10^{-8}\,\mathrm{kg}$, so $\gamma_{\max}(m) = K/m$.

*a. Composite bodies.* A macroscopic body is not a single degree of freedom. In rigid translation at speed $v$, its co-moving constituents (nucleons, nuclei, electrons) each carry energy $E_i = \gamma m_i c^2$ and, if the MDR bound applies per constituent, must satisfy $E_i \le E_{\max}$, giving a bulk limit

$$\gamma \le \min_i \frac{E_{\max}}{m_i c^2}. \quad \text{(B3)}$$

For ordinary matter the tightest bound is set by the heaviest mandatory constituent (e.g., a nucleon), yielding $\gamma_{\max} \sim 4.1 \times 10^{19}$ for $\Delta = t_P$. This is enormous, so at low speeds the MDR is indistinguishable from SR.

*b. Sanity checks.* For an electron, $\gamma_{\max} \sim 7.5 \times 10^{22}$; for a proton, $\sim 4.1 \times 10^{19}$; for a 1 kg bulk mass treated incorrectly as a single mode, $\gamma_{\max} \sim 6.8 \times 10^{-8}$—which is unphysical for bulk kinematics and precisely why the MDR must be applied per constituent.

*c. Inset scale.* Near $v/c = 1$, $1 - v/c \approx 1/(2\gamma^2)$. The horizontal scale of the inset in Fig. 2 is therefore chosen from $\gamma_{\max}$ via $\delta \equiv |1 - v/c| \sim 1/(2\gamma_{\max}^2)$; using a nucleon mass places the ramp in the $10^{-40}$ range, while an ultralight constituent (e.g., $\mu\mathrm{eV}/c^2$) would push it toward $10^{-68}$.

*d. Alternatives.* Other modeling choices (e.g., capping kinetic energy instead of total energy, or using an effective $\Delta$ per microscopic mode) are distinct theories and are not adopted here.


[1] J. C. Spinelli, Finite lorentz factor from discrete proper-time quantization: modified dispersion relation and phenomenology (2025), engrXiv preprint.

[2] J. C. Spinelli, Quantum fields on discrete proper time: Vacuum stress–energy corrections, non-equilibrium phenomenology, and experimental targets (2025), engrXiv preprint, Version 1.

[3] S. W. Hawking and G. F. R. Ellis, *The Large Scale Structure of Space-Time* (Cambridge University Press, 1973).

[4] A. Ashtekar, Phys. Rev. Lett. **57**, 2244 (1986).

[5] C. Rovelli and L. Smolin, Phys. Rev. Lett. **61**, 1155 (1988).

[6] J. Polchinski, *String Theory* (Cambridge University Press, 1998).

[7] N. D. Birrell and P. C. W. Davies, *Quantum Fields in Curved Space* (Cambridge University Press, 1982).

[8] L. Collaboration, Phys. Rev. Lett. **133**, 071501 (2024).

[9] R. Yang, X. Bi, and L. Yin, Timing analysis of grb 221009a with km2a+wcda, LHAASO analysis report (2023).

[10] S. Xi *et al.*, Constraints on lorentz invariance violation from grb 221009a using the discan method (in preparation) (2025).

[11] M. Chen *et al.*, Gamma-ray bursts multi-band constraints on quadratic liv, arXiv:2412.07625 (2024).

[12] A. Ashtekar *et al.*, *Loop Quantum Gravity: The First 30 Years* (World Scientific, 2023).

[13] M. Bojowald, Phys. Rev. Lett. **86**, 5227 (2001).

[14] L. Bombelli, J. Lee, D. Meyer, and R. Sorkin, J. Phys. A: Math. Gen. **20**, 6213 (1987).

[15] G. Amelino-Camelia, Nature **398**, 216 (1999).

[16] F. Fazzini *et al.*, Phys. Rev. D **111**, 046025 (2025), 2409.17099.

[17] I. Agullo *et al.*, Thermodynamics of effective loop quantum black holes, arXiv:2504.06964 (2025).

[18] S. Weinberg, Rev. Mod. Phys. **61**, 1 (1989).

[19] N. Aghanim and others (Planck Collaboration), Astron. Astrophys. **641**, A6 (2020).

[20] D. Collaboration, Desi dr2 results ii: Measurements of baryon acoustic oscillations from the first three years of observations, arXiv:2503.14738 (2025).

[21] S. M. Brewer *et al.*, NIST News (2025), july 14, 2025; accuracy to 19th decimal place.

[22] R. Abbott and others (LIGO-Virgo-KAGRA Collaboration), Gwtc-4.0: Updated gravitational-wave catalog released, LIGO Lab News (2025), august 26, 2025; O4 extended to Nov 18, 2025.

[23] J. C. Spinelli, Numerical kernels for general relativity mdr (jupyter notebook) (2025), open GitHub repository with full reproducible code.